

# Systematics of one-loop Yang–Mills diagrams from bosonic string amplitudes

**Alberto Frizzo and Lorenzo Magnea\***

*Dipartimento di Fisica Teorica, Università di Torino  
and I.N.F.N., Sezione di Torino  
Via P. Giuria 1, I-10125 Torino, Italy*

**Rodolfo Russo**

*Laboratoire de Physique Théorique de l'Ecole Normale Supérieure  
24 rue Lhomond, F-75231 Paris Cedex 05, France*

## Abstract

We present a general algorithm to compute off-shell, one-loop multigluon Green functions using bosonic string amplitudes. We identify and parametrize the regions in the space of moduli of one-loop Riemann surfaces that contribute to the field theory limit of string amplitudes. Each of these regions can be precisely associated with a Feynman-like scalar graph with cubic and quartic vertices, whose lines represent the joint propagation of ghosts and gluons. We give a procedure to compute the contribution of each graph to a gluon Green function, for arbitrarily polarized off-shell gluons, reducible and irreducible diagrams, planar and non-planar topologies. Explicit examples are given for up to six gluons.

---

\*e-mail: magnea@to.infn.it

# 1 Introduction

The fact that string techniques can be used to compute on-shell scattering amplitudes in Yang–Mills theory at tree level [1, 2] and one loop [3, 4, 5] has been known for many years, and has inspired the developments of novel techniques also in field theory [6]. There are several reasons, both from the point of view of strings and in view of further applications to Yang–Mills theory, that lead to consider the extension of this formalism to off-shell correlation functions.

In the context of string theory, it is generally accepted that the framework developed so far for the calculation of scattering amplitudes corresponds to a first-quantized theory, and is properly suited only for on-shell quantities; a consistent extension off the mass-shell of string-derived amplitudes in the field theory limit would provide a non-trivial testing ground for proposals to compute off-shell amplitudes in the full string theory [7]. Recently, similar techniques have been applied also to a non-commutative generalization of field theory [8].

In the context of particle theory, there are several points of interest in going off-shell. First, only with off-shell gluons one can make a definite identification of the gauge selected by string theory; this issue was addressed shortly after the first complete one-loop computations [9], and a combination of gauges that would reproduce the simplifying features of the string calculation was identified. This identification was confirmed in Refs. [10, 11], where a consistent prescription to continue off-shell the string amplitude was proposed, and it was shown that divergent parts of one-loop diagrams were consistent with the identification made in [9]. A general argument detailing how the string amplitude splits into particle graphs, and proving that all such off-shell graphs correspond to a definite gauge, including finite contribution, was however still missing. A second motivation is provided by the desire to extend the string formalism to diagrams with more loops: although partial progress has been made, in the context of scalar amplitudes [12, 13, 14], and for the simplest gluon diagrams [15], tackling a general two-loop gluon amplitude has proved difficult [16]. The main source of this difficulty is the fact that there are several simplifying features of one-loop string calculations that are not preserved by a two-loop generalization: at one loop, for example, it is possible to use partial integration at the string level to eliminate completely the regions of integration corresponding to four point vertices, and furthermore the topology of the graphs contributing non-trivially to the amplitude is essentially unique. At two loops, it

becomes necessary to understand in detail how string moduli space degenerates into a set of graphs in the field theory limit, and the study of scalar diagrams [13] has shown that the reconstruction of Feynman graphs from contributions arising from different regions of moduli space is non-trivial. To solve the problems that arise at two loops, it is then necessary to develop a more systematic approach to the study of the field theory limit; in particular, it is necessary to identify precisely the regions of integration corresponding to particle graphs of various topologies and vertex structures. This can be done consistently only off the mass shell, with a precise identification of the gauge choice, because in Yang–Mills theory the contributions of different graphs mix when the gauge is changed, and the differences only cancel when one sums graphs to reconstruct a gauge-invariant quantity. As a final motivation, it should be emphasized that in Yang–Mills theory and in QCD there are many quantities of theoretical and phenomenological interest that are defined off the mass shell; it would be interesting to apply string techniques to these quantities as well.

In the present paper we will perform a systematic study, of the kind just described, for one-loop Yang–Mills amplitudes. Starting from the string master formula for one-loop gluon amplitudes, we will give a precise characterization of all the regions of integration contributing to the field theory limit. Each such region corresponds to a Feynman-like graph, where, however, the color algebra, the Lorentz algebra, and the loop momentum integration have already been performed; because of this, we will refer to such a graph as a ‘scalar graph’. One-loop scalar graphs correspond to sums of Feynman diagrams, since both gluons and ghosts circulate in the loop. Scalar graphs in general contain both cubic and quartic vertices, and can be one-particle reducible or irreducible, as well as planar or non-planar. We will give examples of each kind: in particular, we will consider in detail the case of diagrams with quartic vertices, which arise from integration over finite regions in string moduli space, and in some cases require a regularization of infrared singularities arising from the propagation of bosonic string tachyons in intermediate channels.

The string master formula, when applied to off-mass-shell, non-transverse external gluons, depends on a set of projective transformations (one for each external state), defining a local coordinate system on the world-sheet around the point of insertion of each external particle. At one loop, geometrical arguments lead to an

essentially unique choice of these projective transformation that preserves the global properties of the geometric objects appearing in the string master formula<sup>1</sup>. We will show that, in each of the cases examined, this choice leads to a well-defined off-shell continuation of the amplitude, which corresponds to the combination of gauges described in Refs. [9] and [11]. The correspondence is apparent at the level of the integrands when the amplitude is expressed in terms of Schwinger or Feynman parameters, so it can be checked case by case without having to perform any integration. Since the results are valid for external gluons with arbitrary mass and polarization, polarization vectors could be dropped and the results could be read directly as the values of the corresponding truncated Green functions, expressed as functions of the external momenta.

We emphasize that, although a precise correspondence between scalar graphs arising from string theory and sets of diagrams in field theory is established, it remains true that the string method is vastly convenient from a practical point of view, essentially because it generates automatically the answer for the sum of a subset of diagrams *after* loop momentum integration, directly in terms of external momenta and polarizations, bypassing all intermediate stages of the calculation, in which typically hundreds of thousands of terms are generated. We emphasize also that, in its present form, the method lends itself to be completely automated, in the sense that all expressions for the integrands of all relevant scalar graphs can be machine-generated in a short time starting from the basic string ingredients. The only obstacle remaining on the way to a complete calculation is the computation of scalar integrals, something for which this approach can offer no help.

The paper is organized as follows. In Section 2, we introduce the necessary ingredients of the string formalism, we explain the role of projective transformations, and give the geometric prescription for the off-shell continuation. In Section 3 we describe the general features of the procedure used to take the field theory limit, introducing the mapping between string moduli and Schwinger parameters in field theory. In Section 4, we focus on the regions in moduli space corresponding to diagrams with cubic vertices only; we give examples of 3 and 4 point diagrams and specifically of a non-planar contribution. In Section 5, we show how to treat quartic vertices, defining the necessary regularization prescriptions. In Section 6 we

---

<sup>1</sup>A choice of this kind was proposed in Ref. [7], where results similar to ours were obtained for the two- and the three-point functions.

turn our attention to reducible diagrams, and verify the non-trivial gauge choice performed by the string in this case. In Section 7 we summarize our calculational method, which is now as general and systematic as conventional Feynman rules, at least for one-loop correlation functions, and we give a concrete example of the application of the method to a more complicated graph, computing a contribution to the six-gluon one-loop amplitude. Finally, in Section 8, we draw our conclusions and discuss possible developments and applications.

## 2 The one-loop off-shell master formula

Open bosonic string theory is the simplest string model containing a massless vector state. Of course, the whole spectrum consists of an infinite tower of states with masses proportional to the string tension  $T$ ; however, all the contributions to scattering amplitudes coming from massive modes disappear in the low-energy limit,  $T \rightarrow \infty$ , and the dynamics of the surviving light modes can be effectively described by a field theory. As discussed in Ref. [13], it is possible to reproduce different field theories in the infinite tension limit by choosing different matching conditions for the coupling. Here we will be concerned with the Yang-Mills field theory limit (first discussed in Ref. [4]), which is obtained by allowing the circulation of only massless states in the loop.

There are two potential technical problems in the computation of the Yang-Mills field theory limit: the fact that the ground state of the spectrum of the bosonic string is a tachyon, and the fact that string amplitudes are computed in the critical dimension  $d = d_c = 26$ . Neither problem affects the result: it turns out that tachyonic contributions to gluon amplitudes correspond to infrared divergences that can be easily identified and regulated by hand, and furthermore one can continue the string amplitude to arbitrary values of  $d \neq 26$ , obtaining in fact the correct result for the dimensionally regularized field theory of interest.

The continuation to arbitrary  $d$  can be justified from the point of view of string theory by constructing a simple, though consistent, string model, having as low-energy limit the pure  $d$ -dimensional Yang-Mills theory [17]. It is sufficient to break the full 26-dimensional Lorentz invariance by imposing different boundary conditions on the open string along different directions. Since we want open strings to be free to move in  $d$  of the original 26 dimensions, we split our space time as

$\mathcal{M}_{26} = M_d \times \mathcal{M}_{26-d}$ , where  $M_d$  is  $d$ -dimensional Minkowsky space; then we choose Neumann boundary conditions along  $M_d$  and Dirichlet boundary conditions along  $\mathcal{M}_{26-d}$ ; in other words, we consider a bosonic  $D(d-1)$ -brane. It is well known that the massless sector of such open strings also contains states which are scalars from the  $d$ -dimensional point of view. In order to decouple these unwanted scalars, one can choose  $\mathcal{M}_{26-d}$  to be the orbifold  $\mathbf{R}^{26-d}/Z_2$ , where the  $Z_2$  orbifold operation is simply the reflection in  $\mathbf{R}^{26-d}$  around the origin. The orbifolded theory must contain only the open string states which are invariant under  $Z_2$ . By choosing a trivial action of this  $Z_2$  operation on the Chan–Paton factor, it is easy to see that all the massless scalar are projected out by the orbifold operation, and one is left with a pure  $d$ -dimensional Yang–Mills theory (in the  $D$ -brane language, we are using bosonic ‘fractional branes’). The use of this kind of  $D$ -branes, present in orbifolded theories, is a quite general technique for generating pure Yang–Mills theory also in the supersymmetric case.

Of course, the string master formula one derives in the orbifold model would be more complicated than the one presented here, in Eq. (2.2). However, as long as one considers scattering amplitudes only among vector states, the differences conspire precisely, in the field theory limit, to change the effective value of the dimension from  $d_c = 26$  to  $d$  [17]. Thus, computing the string amplitudes from Eq. (2.2) directly in  $d$  dimensions is, at one loop and in the field theory limit, a shortcut perfectly equivalent to the computation in the orbifolded model in the critical dimension. The gluon amplitude computed this way automatically has the correct  $d$  dependence, and thus is given in dimensionally regularized form. This also provides a simple criterion to identify tachyonic contributions: they are in fact infrared divergent in the field theory limit for all values of  $d$ , *i.e.* they are not regularized by dimensional continuation. Such contributions must be discarded, just as the contributions of massive states, although they may leave finite remainders after regularization, as we will see in Section 5.

A further technical problem of special relevance to the present paper is the fact that string amplitudes must be computed between states satisfying the mass–shell condition, to preserve conformal invariance on the string world–sheet. It turns out, however, that the effects of off–shell continuation are parametrized in a simple way in the context of the operator formalism [18]: the amplitude acquires a dependence on a set of projective transformations defining local coordinate systems around the

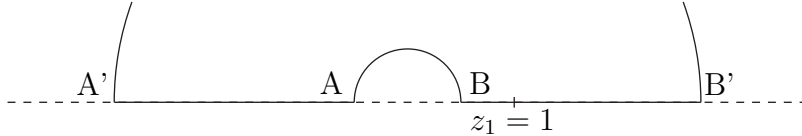


Figure 1: The annulus in Schottky representation.

locations of the insertions of external gluons. As we will see, there is a simple, geometrically motivated choice for these projective transformations, which consistently yields the correct off-shell extension for Yang–Mills amplitudes.

Since our aim here is to provide a self-contained method to calculate gluon diagrams, we will not emphasize technical details of the string formalism, which are available elsewhere [18, 19]. We will just give the general expression for the one-loop multigluon string amplitude, and describe the geometric features necessary to define and perform the field theory limit.

It should be kept in mind that string theory, although describing the propagation of objects in a  $d$ -dimensional space time, has a two-dimensional structure describing the world-sheet dynamics. Thus the amplitudes for the scattering of string states, and the ingredients entering in their expression, must have a meaning also from the point of view of the two-dimensional theory. String amplitudes must then be written in the language of Riemann surfaces, in our case with boundaries and punctures representing the insertions of external gluons. Using the operator formalism [18], Riemann surfaces turn out to be represented in the Schottky parametrization [20], which is the one we will use. In particular, one-loop open string amplitudes involve insertions of gluon vertex operators on the boundaries of an annulus, which, in the Schottky parametrization, is represented as in Fig. 1.

The boundaries of the annulus correspond to the segments  $AA'$  and  $BB'$ , whose endpoints must be identified. External gluons will be inserted on the boundaries at locations  $z_i$ , often referred to as ‘punctures’. It is easy to see how the idea of adding loops is implemented in this formalism. One starts from the upper half complex

plane (equivalent to the disk, representing the tree–level scattering amplitude), and adds two circles with centers on the real axis, which must then be identified via a projective transformation. Each loop is thus characterized by three real parameters: the positions of the two centers on the real axis and the common radius of the circles, which fix respectively the positions and the width of the holes added to the surface. The positions of the various circles are related to the fixed points of the projective transformations under which the pairs of circles are identified. Usually the fixed points are denoted by  $\xi$  and  $\eta$ , while the width of the holes is determined by the third parameter characterizing the projective transformation, the multiplier  $k$ . The fundamental building block entering the amplitudes is the Green function of the two–dimensional Laplace operator defined on the string world–sheet, denoted by  $\mathcal{G}(z_i, z_j)$ : it is the correlator of two world–sheet bosons located at positions  $z_i$  and  $z_j$  and of course depends on the parameters  $(\xi, \eta, k)$  defining the Riemann surface.

At this point we can write down the ‘master formula’ for the one–loop multi–gluon string amplitude, in terms of the Green function  $\mathcal{G}$ . If one does not impose the mass–shell and transversality conditions on the external states, the Green function must be evaluated in terms of the projective transformations associated with the punctures, denoted by  $V_i(z)$ , which must satisfy

$$V_i(0) = z_i , \quad (2.1)$$

in order to define local coordinates around  $z_i$ . The master formula is then given by

$$\begin{aligned} A^{(1)}(1, \dots, M) &= \text{Tr}(\lambda^{a_1} \dots \lambda^{a_m}) \text{Tr}(\lambda^{a_{m+1}} \dots \lambda^{a_M}) \frac{2^M g_S^M}{(2\pi)^d} (2\alpha')^{(Md-2M-2d)/4} \\ &\times \int \frac{\prod_{i=1}^M dz_i}{dV_{abc} V_i'(0)} \frac{dk d\xi d\eta}{k^2(\xi - \eta)^2} \left(-\frac{\ln k}{2\pi}\right)^{-d/2} \prod_{n=1}^{\infty} (1 - k^n)^{2-d} \\ &\times \left\{ \exp \left[ \frac{1}{2} \sum_i \sqrt{2\alpha'} p_i \cdot \epsilon_i \left( \frac{V_i''(0)}{V_i'(0)} \right) \right] \prod_{i < j} \left[ \frac{\exp(\mathcal{G}(V_i(z), V_j(y)))}{\sqrt{V_i'(z) V_j'(y)}} \right]_{z=y=0}^{2\alpha' p_i \cdot p_j} \right. \\ &\times \exp \left[ \sum_{i \neq j} \left( \sqrt{2\alpha'} p_j \cdot \epsilon_i [\partial_z \mathcal{G}(V_i(z), V_j(y))]_{z=y=0} \right. \right. \\ &\left. \left. + \frac{1}{2} \epsilon_i \cdot \epsilon_j [\partial_z \partial_y \mathcal{G}(V_i(z), V_j(y))]_{z=y=0} \right) \right] \Big\}_{\text{m.l.}} , \quad (2.2) \end{aligned}$$

where the subscript ‘‘m.l.’’ means that only terms multilinear in all polarization vectors must be considered.



Eq. (2.2) gives the one-loop contribution to the color-ordered scattering amplitude of  $M$  gluons characterized by momenta  $p_i$ , polarization vectors  $\epsilon_i$  and color indices  $a_i$ , in the general case in which the mass-shell ( $p_i^2 = 0$ ) and transversality ( $\epsilon_i \cdot p_i = 0$ ) conditions have not been imposed<sup>2</sup>. Since this amplitude is color-ordered (one needs to sum over all inequivalent orderings, to obtain the full amplitude), the color structure is factorized and appears in the form of a Chan–Paton factor. At one loop this factor contains at most two traces of color matrices, corresponding to the insertion of gluons on both boundaries of the annulus; in the planar case one has  $m = 0$ , and only one trace survives, multiplied times a factor of  $N = \text{Tr}\mathbf{1}$ . The string coupling  $g_S$  can be related to the gauge coupling in  $d = 4 - 2\epsilon$  dimensions by matching the values of the tree-level three-point amplitude derived from string theory with the corresponding Yang–Mills Feynman rule. With our choice of normalization for the the  $SU(N)$  generators in the fundamental representation,  $\lambda^a$ ,

$$\text{Tr}(\lambda^a \lambda^b) = \frac{1}{2} \delta^{ab} , \quad (2.3)$$

the matching condition reads [11]

$$g_S = \frac{g_d}{2} (2\alpha')^{1-d/4} , \quad (2.4)$$

where  $g_d = g_{YM} \mu^\epsilon$ , and  $\alpha'$ , the Regge slope, is inversely proportional to the string tension  $T$ . In the field theory limit one considers amplitudes where the typical energy is much smaller than  $\alpha'^{-1/2}$ , that is  $\alpha' p_i \cdot p_j \ll 1$ . This limit can be computed by formally considering  $\alpha' \rightarrow 0$ .

The Koba–Nielsen variables  $z_i$  in Eq. (2.2) represent the locations of gluon insertions on the boundary of the one-loop world-sheet. The symbol  $dV_{abc}$  in the integration measure reminds us that projective invariance of the string amplitude can be used to fix the location of three integration variables, chosen among the punctures  $z_i$  or the fixed points. Multipliers, on the other hand, cannot be fixed; as we will see, they are related to Schwinger parameters measuring the total length of the loops. In the present case, it is convenient to fix  $\xi = \infty$ ,  $\eta = 0$ ; next, we fix the position of one of the punctures, setting  $z_1 = 1$ , as indicated in Fig. 1.

The dependence of Eq. (2.2) on the projective transformations  $V_i(z)$  deserves further comment. Local coordinates around the punctures must be introduced in the operator formalism in order to perform the sewing procedure [18], which leads to

---

<sup>2</sup>Notice that we use the metric  $(-+++)$  in string-derived expressions.

the construction of loop amplitudes from a tree-level multi-leg vertex operator (the ‘ $N$ -Reggeon vertex’)<sup>3</sup>. If one imposes the mass-shell and transversality conditions, it can be easily verified that the  $V_i$  dependence in Eq. (2.2) cancels, as a consequence of momentum conservation. Furthermore, as we will see, even off-shell it is possible to reabsorb all the  $V_i$  dependence in a simple redefinition of the Green function. This can be achieved by defining

$$G(V_i(z), V_j(y)) = \mathcal{G}(V_i(z), V_j(y)) - \frac{1}{2} \log |V'_i(z)| - \frac{1}{2} \log |V'_j(y)| . \quad (2.5)$$

Substituting Eqs. (2.4) and (2.5) into Eq. (2.2), and making use of Eq. (2.1), we recover a simpler expression of the master formula, which was used in previous work [11], and which has no explicit dependence on the projective transformations  $V_i(z)$ . What is most significant is the fact that the term proportional to  $p_i \cdot \epsilon_i$  is canceled *without* imposing the transversality condition to external gluons. The formula we find is then applicable to unphysical as well as to physical polarizations. Focusing on the planar case, the ‘practical version’ of the master formula can be written as

$$\begin{aligned} A_P^{(1)}(1, \dots, M) &= N \operatorname{Tr}(\lambda^{a_M} \dots \lambda^{a_1}) \frac{g_d^M}{(4\pi)^{d/2}} (2\alpha')^{(M-d)/2} \int_0^1 \frac{dk}{k^2} \prod_{n=1}^{\infty} (1 - k^n)^{2-d} \\ &\times \int_k^1 dz_M \int_{z_M}^1 dz_{M-1} \dots \int_{z_3}^1 dz_2 \left( -\frac{\log k}{2} \right)^{-d/2} \prod_{i < j} \left( \exp [G(z_i, z_j)] \right)^{2\alpha' p_i \cdot p_j} \quad (2.6) \\ &\times \left\{ \exp \left[ \sum_{i \neq j} \left( \sqrt{2\alpha'} p_j \cdot \epsilon_i \partial_i G(z_i, z_j) + \frac{1}{2} \epsilon_i \cdot \epsilon_j \partial_i \partial_j G(z_i, z_j) \right) \right] \right\}_{\text{m.l.}} . \end{aligned}$$

To extract results from Eq. (2.6) in the case of off-shell gluons, one must of course make a choice for the  $V_i(z)$ . This choice can be guided by two-dimensional geometry. It is known in fact that, for any Riemann surface, the Green function contains the logarithm of the prime form, which is essentially a well defined analytic generalization of the monomial  $z_i - z_j$  to higher-genus surfaces. The prime form is not a function on the surface, but rather a differential form of weight  $\{-1/2, -1/2\}$ . One sees from Eq. (2.5) that one can construct a well behaved Green function on the surface by choosing the  $V_i(z)$ ’s so that their derivatives  $V'_i(0)$  behave as differential forms of weight  $-1$ . The only globally defined one-forms on a genus  $g$  Riemann

---

<sup>3</sup>Roughly speaking, the sewing procedure generates a  $g$ -loop,  $m$ -point amplitude by inserting a propagator between two external states of a  $(g-1)$ -loop,  $(m+2)$ -point amplitude, and summing over the whole spectrum of string states propagating in that channel.

surface are the  $g$  abelian differentials, so, at one loop, this criterion leads to an essentially unique choice. One must choose

$$V'_i(0) = (\omega(z_i))^{-1} , \quad (2.7)$$

where  $\omega(z)$  is related to the unique abelian differential on the torus, which for our choice of fixed points ( $\xi = \infty$ ,  $\eta = 0$ ) is simply  $dz/z$ . We are lead uniquely to the choice  $V'_i(0) = z_i$ , already adopted in Refs. [11, 13]. With this choice, the modified open string Green function  $G(z_i, z_j)$  defined in Eq. (2.5) is given by

$$\begin{aligned} G(z_i, z_j) &= \log \left( \left| \sqrt{\frac{z_i}{z_j}} - \sqrt{\frac{z_j}{z_i}} \right| \right) + \frac{1}{2 \log k} \left( \log \frac{z_i}{z_j} \right)^2 \\ &+ \log \left[ \prod_{n=1}^{\infty} \frac{\left( 1 - k^n \frac{z_j}{z_i} \right) \left( 1 - k^n \frac{z_i}{z_j} \right)}{(1 - k^n)^2} \right] ; \end{aligned} \quad (2.8)$$

notice that  $G(z_i, z_j)$  is actually a function only of the ratio  $\rho_{ij} = z_i/z_j$ , so that it is translationally invariant on the torus parametrized by coordinates  $\nu_i \sim \log(z_i)$ .

We conclude this section with a comment on the integration region over the moduli given in Eq. (2.6). Notice that the  $z_i$ 's are ordered between  $k$  and  $z_1 = 1$ . In fact, in the Schottky parametrization, for a planar configuration, all punctures are constrained to lie on the same boundary of the string world-sheet, thus, having fixed  $z_1 = 1$ , all other  $z_i$  should be integrated over the interval  $B = \sqrt{k} < z_i < B' = 1/\sqrt{k}$ , with the restriction on the ordering implied by the color trace. This would complicate the calculation of the field theory limit, since there would be contributions both from  $z_i \rightarrow \sqrt{k} \rightarrow 0$  and from  $z_i \rightarrow 1/\sqrt{k} \rightarrow \infty$ . It is possible to bypass this practical difficulty by making use of the fact that the string integrand is modular invariant, which in particular implies that the interval  $[1, 1/\sqrt{k}]$  can be mapped onto the interval  $[k, \sqrt{k}]$ . One can easily show that the effective one-loop Green function in Eq. (2.5) satisfies

$$\begin{aligned} G(\rho_{ji}; k) &= G(\rho_{ij}; k) \\ G(k\rho_{ji}; k) &= G(\rho_{ij}; k) , \end{aligned} \quad (2.9)$$

where  $\rho_{ij} = z_i/z_j$  and with a slight abuse of notation we write  $G(\rho_{ij}; k) \equiv G(z_j, z_i)$ . Using these properties, one can map all configurations with a subset of punctures in the interval  $[1, 1/\sqrt{k}]$  to configurations in which those punctures have been moved to the interval  $[k, \sqrt{k}]$ , preserving the ordering on the circle. This procedure yields the integration region in Eq. (2.6).

### 3 General structure of the field theory limit

In the formal limit  $\alpha' \rightarrow 0$ , Eq. (2.6) gives a vanishing or a divergent result, depending on the number of external gluons,  $M$ . It is clear that a finite result can be obtained only by considering singular regions of integration, and parametrizing the singularities in order to generate powers of  $\alpha'$ , to compensate the explicit factor of  $\alpha'^{(M-d)/2}$ . In order to do this, it will be necessary to change integration variables from the dimensionless quantities  $\{k, z_i\}$  to dimensionful parameters characterizing the size and shape of the string world-sheet in units of  $\alpha'$ .

The appropriate change of variables is once again suggested by the geometric structure emerging from the operator formalism. The sewing procedure, in fact, indicates that when the integrand of Eq. (2.6) is written out as a Laurent series expansion in powers of the multiplier  $k$ , the coefficient of  $k^n$  represents the contribution to the amplitude due to the circulation in the loop of states belonging to mass level  $n + 1$ . Since the integrand has no power-law divergence as  $k \rightarrow 0$ , except the explicit factor of  $k^{-2}$ , one can conclude that the terms proportional to  $k^{-2}$  correspond to tachyon propagation (mass level  $n = -1$ ), while the contribution of gluons (mass level  $n = 0$ ) will be given by terms proportional to  $k^{-1}$ . This interpretation of the role played by  $k$  also rules out the possibility of expressing  $k$  directly as the ratio of a dimensionful parameter and  $\alpha'$ ; furthermore, after isolating the correct power of  $k$ , the only singularities left in the integrand are logarithmic, and the measure of integration for the multiplier is just  $d \log k$ . This suggests [21] that one should identify the logarithm of the multiplier with the length of the string loop, measured in units of  $\alpha'$ , in agreement with the fact that the limit  $k \rightarrow 0$  corresponds to a very long and narrow annulus, as seen explicitly in Fig. 1. It is then natural to think of the puncture coordinates as associated to fractional lengths in a similar way. This leads to the choice

$$\log k = -\frac{t}{\alpha'} , \quad \log z_i = -\frac{t_i}{\alpha'} , \quad (3.1)$$

which has been employed in the past for both gluon [3, 11] and scalar [13] amplitudes. It turns out that the variables  $t_i$  and  $t$  play the role of Schwinger parameters associated to combinations of field theory propagators, as we will see explicitly below.

Once the change of variables in Eq. (3.1) has been effected, the field theory limit can be reached by taking  $\alpha' \rightarrow 0$  with  $\{t, t_i\}$  fixed. Thus one expands the integrand

of Eq. (2.6) in powers of  $k$  and  $z_i$ , retains the coefficients of  $k^{-1}$  and  $z_i^{-1}$ , and keeps all terms that have a finite limit as  $\alpha' \rightarrow 0$ . As we will see, one must be careful to include all sources of  $\alpha'$  dependence, and all singular regions of integration.

This is a representative case of the general strategy that must be employed also for amplitudes with more loops: the zero-slope limit has to be taken after introducing the dimensionful field theory variables that have to be kept fixed. The exact form of the change of integration variables identifies the particular corner of moduli space being considered. To get the complete result, it is necessary to make sure that all singular corners of integration have been taken into account. In particular, in the case of one-loop gluon amplitudes, it is immediately clear that the region identified by Eq. (3.1) cannot give the complete answer. Consider in fact the counting of powers of  $\alpha'$  in Eq. (2.6) after implementing Eq. (3.1): one finds an overall factor of  $(\alpha'/2)^{-M/2}$  from the normalization and the change of variables, and a further factor of  $\alpha'^m$ , with  $0 \leq m \leq M/2$ , from the terms multilinear in the polarization vectors arising from the expansion of the second exponential. Specifically, only the terms containing no double derivatives of the Green function display a complete cancellation of the overall power of  $\alpha'$ , giving immediately a contribution to the field theory limit. All terms containing double derivatives of  $G$  still have an overall *negative* power of  $\alpha'$ , and one must find further sources of positive powers of  $\alpha'$  in order to generate finite contributions from these terms. There are two such sources, which generate classes of contributions which are easily identified in the field theory limit.

- Positive powers of  $\alpha'$  will arise from regions of integration in which certain Schwinger parameters are small, in fact are themselves  $\mathcal{O}(\alpha')$ . Notice that so long as, say,  $t_i < t_j$ , in the  $\alpha' \rightarrow 0$  limit the punctures are strongly ordered on the real axis, *i.e.*  $z_j \ll z_i$ . Taking  $t_i - t_j = \mathcal{O}(\alpha')$ , on the other hand, means that the punctures remain close to each other as the field theory limit is taken. These integration regions must then, and do, correspond to four-point vertices in field theory. From the point of view of string theory such contributions only arise naturally in gluon amplitudes: if one takes a field theory limit corresponding to scalars with a cubic coupling, these regions are always suppressed by powers of  $\alpha'$ . Notice also that the counting of powers of  $\alpha'$  described above correctly reproduces the counting of four-point vertices in gluon diagrams: in an  $M$ -point one-loop amplitude there can be at most  $M/2$

four–point vertices (or  $(M - 1)/2$ , for odd  $M$ ), which is also the maximum number of powers of  $\alpha'$  that can be extracted with this method in Eq. (2.6) without getting a vanishing result. For obvious dimensional reasons, diagrams with only four–point vertices have no powers of momenta in the numerator, and thus give results in which all polarization vectors are dotted into each other; this is also directly evident in Eq. (2.6).

- A second source of positive powers of  $\alpha'$  is the first exponential factor of Eq. (2.6). In fact, upon substituting Eq. (3.1), one easily sees that this factor takes the form

$$\prod_{i < j} [\exp(G(z_i, z_j))]^{2\alpha' p_i \cdot p_j} = \exp(c_0(t_i) + \alpha' c_1(t_i)) . \quad (3.2)$$

Clearly, if the overall power of  $\alpha'$  in Eq. (2.6) is negative, Eq. (3.2) must be expanded as

$$\prod_{i < j} [\exp(G(z_i, z_j))]^{2\alpha' p_i \cdot p_j} = \exp(c_0(t_i)) \left( 1 + \alpha' c_1(t_i) + \frac{1}{2} \alpha'^2 c_1(t_i)^2 + \dots \right) , \quad (3.3)$$

and thus participates in the counting of  $\alpha'$ . All terms arising from diagrams containing only cubic vertices but containing factors of the form  $p_i \cdot p_j \dots \epsilon_k \cdot \epsilon_l$  are generated by string theory through this expansion.

The discussion developed so far is based upon the idea of expanding the integrand in powers of  $k$  and  $z_i$ , assuming that the punctures are not too close to each other, so that the Green function is not dominated by its short distance singularity as  $z_i \rightarrow z_j$ . As a result, one gets all 1PI contributions to the amplitude. As pointed out long ago [3], one can also get one–particle–reducible contribution, by considering the opposite limit, taking  $z_i \rightarrow z_j$  *before* the field theory limit, driven by  $k \rightarrow 0$ . This procedure is also a source of powers of  $\alpha'$ , since it generates dimensionless gluon propagators in the chosen channel, in the form  $1/(\alpha' p_i \cdot p_j)$ . This limit will be discussed in more detail in Section 6.

Summarizing, we have tentatively identified all the regions of integration in moduli space contributing to the field theory limit. We see that in this limit the string amplitude decomposes into a sum of contributions associated to graphs that, as we shall see, are in straightforward correspondence with the Feynman graphs of the limiting field theory. Specifically, the graphs for a given amplitude can be

enumerated by counting the Feynman graphs with the same number of external legs in a scalar theory with both cubic and quartic interactions. Each string-derived graph corresponds to a sum of Feynman graphs in Yang–Mills theory, involving the propagation of both ghosts and gluons. Furthermore, the field theory limit yields directly the Schwinger parameter integral, having bypassed all Lorentz and color algebra, loop momentum integration, and the decomposition of tensor integrals into scalar building blocks [23, 24]. We will refer to the string-derived graphs as ‘scalar graphs’. Scalar graphs are directly expressed in terms of scalar integrals, albeit with a numerator structure reminiscent of the presence of momenta in Yang–Mills vertices. At least at one loop, string theory effectively succeeds in reducing the complexity of the calculation of a Yang–Mills amplitude to a level close to a scalar amplitude, even in the general case of off-shell gluons with arbitrary polarizations.

In the next sections, we will describe in more detail how different scalar graphs must be computed starting from Eq. (2.6). We will consider in turn irreducible graphs with only cubic vertices, arising from the region in which the punctures are strongly ordered (Section 4), then irreducible graphs with quartic vertices, arising when the strong ordering condition is relaxed (Section 5), and finally reducible graphs (Section 6). In each case we will give concrete examples. Because the graphs are computed with off-shell gluons, their values are gauge-dependent in field theory. One is then able to make a precise identification of the gauge choice made by string theory, and in fact our calculations confirm the results of Refs. [9] and [11]: the string computes the amplitudes in a combination of the background Feynman gauge (for irreducible diagrams) with the Gervais–Neveu gauge (for trees attached to the loop). It is tempting to identify the dependence of the off-shell string amplitude on the choice of projective coordinates  $V_i'(0)$  with a gauge dependence in the field theory limit. However we have so far been unable to make this identification precise.

We conclude this section by listing the explicit expressions that we will need for the Green function and its derivatives in the various relevant limits. In the limit  $k \rightarrow 0$ , Eq. (2.8) and its derivatives have the expansions

$$\begin{aligned}
G(\rho_{ij}; k) &= \log(1 - \rho_{ij}) - \frac{1}{2} \log \rho_{ij} + \frac{\log^2 \rho_{ij}}{2 \log k} - k \left( \rho_{ij} + \frac{1}{\rho_{ij}} - 2 \right) + \mathcal{O}(k^2) , \\
\partial_i G(\rho_{ij}, k) &= \frac{1}{z_j} \left[ -\frac{1}{1 - \rho_{ij}} - \frac{1}{2\rho_{ij}} + \frac{\log \rho_{ij}}{\rho_{ij} \log k} - k \left( -\frac{1}{\rho_{ij}^2} + 1 \right) \right] + \mathcal{O}(k^2) , \\
\partial_j G(\rho_{ij}; k) &= -\frac{z_i}{z_j^2} \left[ -\frac{1}{1 - \rho_{ij}} - \frac{1}{2\rho_{ij}} + \frac{\log \rho_{ij}}{\rho_{ij} \log k} - k \left( -\frac{1}{\rho_{ij}^2} + 1 \right) \right] + \mathcal{O}(k^2) ,
\end{aligned}$$

$$\partial_i \partial_j G(\rho_{ij}; k) = \frac{1}{z_i z_j} \left[ -\frac{1}{\log k} + \frac{\rho_{ij}}{(1 - \rho_{ij})^2} + k \left( \frac{1}{\rho_{ij}} + \rho_{ij} \right) \right] + \mathcal{O}(k^2), \quad (3.4)$$

where  $\rho_{ij} = z_i/z_j < 1$ , since the punctures are radially ordered on the boundary.

As we will see in Section 4, if the two punctures are on different boundaries, so that their coordinates have opposite sign in Schottky parametrization, the Green function is slightly modified and becomes

$$\widehat{G}(\rho_{ij}, k) = \log(1 + |\rho_{ij}|) - \frac{1}{2} \log |\rho_{ij}| + \frac{\log^2 |\rho_{ij}|}{2 \log k} + k(|\rho_{ij}| + \frac{1}{|\rho_{ij}|} + 2) + \mathcal{O}(k^2). \quad (3.5)$$

When considering reducible diagrams, we will also need the limit of the Green function as  $\rho \rightarrow 1$ . In this limit, the logarithmic singularity dominates, and one can use simply

$$G(\rho; k) = \log(1 - \rho) + \mathcal{O}(1 - \rho). \quad (3.6)$$

When the two punctures are on different boundaries, there is no logarithmic singularity in the integration domain, at least when considering three-gluon vertices, so the corresponding limit for the non-planar Green function is not needed. We are now ready to turn to a more detailed analysis of the field theory limit for different scalar graph topologies.

## 4 Irreducible diagrams with cubic vertices

Irreducible scalar diagrams with only cubic vertices are the most straightforward to compute, since they arise naturally from the region of moduli space parametrized by Eq. (3.1) in the limit  $\alpha' \rightarrow 0$ . As pointed out above, in this region each gluon insertion on the annulus is widely separated from the contiguous ones: thus, on both sides of each external state there are loop propagators. Consider, for example, two contiguous punctures  $z_i$  and  $z_{i+1}$ . According to Eq. (3.1), in the field theory limit we set

$$z_i = e^{-t_i/\alpha'} \quad ; \quad z_{i+1} = e^{-t_{i+1}/\alpha'}. \quad (4.1)$$

The existence of a loop propagator between the two insertions, requires that its proper time, *i.e.*  $t_{i+1} - t_i$ , be kept finite as  $\alpha' \rightarrow 0$ . Then

$$\frac{t_{i+1} - t_i}{\alpha'} \rightarrow \infty \quad \Rightarrow \quad \frac{z_{i+1}}{z_i} \rightarrow 0 \quad \Rightarrow \quad z_{i+1} \ll z_i, \quad (4.2)$$



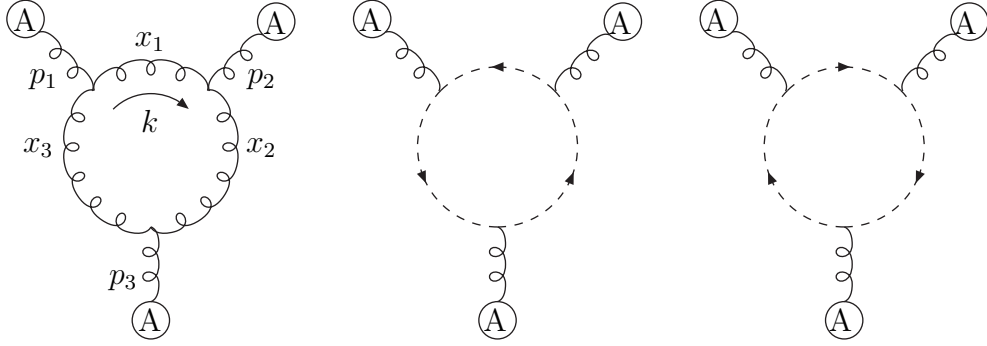


Figure 2: Three-point diagrams: external gluons are background fields, marked by an A. Momenta  $p_i$  are incoming.

thus we conclude that the gluon labeled by  $i$  connects to the loop through a cubic vertex if the Koba-Nielsen variables adjacent to it are strongly ordered,  $z_{i+1} \ll z_i \ll z_{i-1}$ <sup>4</sup>.

To illustrate the technique, we will begin by computing the sum of the three diagrams given in Fig. 2, using Eq. (2.6) for  $M = 3$ , and changing variables according to Eq. (3.1). Concentrating on the color ordering (3-2-1), and retaining only the leading terms in the expansion in powers of the multiplier, Eq. (2.6) for  $M = 3$  reads

$$\begin{aligned}
A^{(1)}(1, 2, 3) &= N \operatorname{Tr}(\lambda^3 \lambda^2 \lambda^1) \frac{g_d^3}{(4\pi)^{d/2}} (2\alpha')^{2-d/2} \int_0^1 \frac{dk}{k^2} \int_k^1 dz_3 \int_{z_3}^1 dz_2 \quad (4.3) \\
&\times \left( -\frac{\log k}{2} \right)^{-d/2} (1 + k(d-2)) \exp \left[ 2\alpha' (p_1 \cdot p_2 G_{12} + p_1 \cdot p_3 G_{13} + p_2 \cdot p_3 G_{23}) \right] \\
&\times \left\{ 2\alpha' (\epsilon_1 \cdot p_2 \partial_1 G_{21} + \epsilon_1 \cdot p_3 \partial_1 G_{31}) (\epsilon_2 \cdot p_3 \partial_2 G_{32} + \epsilon_2 \cdot p_1 \partial_2 G_{12}) \right. \\
&\quad \times (\epsilon_3 \cdot p_1 \partial_3 G_{13} + \epsilon_3 \cdot p_2 \partial_3 G_{23}) \\
&\quad \left. + \left[ \epsilon_1 \cdot \epsilon_2 \partial_1 \partial_2 G_{12} (\epsilon_3 \cdot p_1 \partial_3 G_{13} + \epsilon_3 \cdot p_2 \partial_3 G_{23}) + (cycl.) \right] \right\}.
\end{aligned}$$

Here  $G_{ij}$  denotes the expansion of  $G(\rho_{ij}, k)$  in powers of  $k$ , Eq. (3.4).

To proceed, we note that changing variables to Schwinger parameters the overall

---

<sup>4</sup>We work in the configuration  $0 \leq k \leq z_M \leq \dots \leq z_1 = 1$ . To state that  $z_M$  is widely separated from  $z_1 = 1$ , we may simply require it to be widely separated from  $k$ , since points  $k$  and 1 are identified on the annulus.

power of  $\alpha'$  becomes  $\alpha'^{-1}$ . Thus for the terms in Eq. (4.3) that do not contain double derivatives of the Green function all polynomial dependence on  $\alpha'$  cancels and the field theory limit can be taken directly. The terms proportional to double derivatives of  $G$ , however, need an extra positive power of  $\alpha'$ . This can be supplied by the term proportional to  $1/\log k$  in Eq. (3.4), but to get the complete result for these terms it is necessary to expand the exponential as well, according to Eq. (3.3). Once this is done, the field theory limit can be taken by picking the coefficient of  $\alpha'^0 k^0 z_i^0$  in the resulting polynomial, while the exponential factor becomes simply

$$\begin{aligned} & \exp \left[ 2\alpha' (p_1 \cdot p_2 G_{12} + p_1 \cdot p_3 G_{13} + p_2 \cdot p_3 G_{23}) \right] \rightarrow \\ & \exp \left[ p_1 \cdot p_2 t_2 \left( 1 - \frac{t_2}{t} \right) + p_1 \cdot p_3 t_3 \left( 1 - \frac{t_3}{t} \right) + p_2 \cdot p_3 (t_3 - t_2) \left( 1 - \frac{t_3 - t_2}{t} \right) \right]. \end{aligned} \quad (4.4)$$

To write our final answer in the most symmetric manner, it is convenient to introduce the dimensionless Feynman parameters  $x_1 = t_2/t$ ,  $x_2 = (t_3 - t_2)/t$ ,  $x_3 = 1 - x_1 - x_2$ , and to define  $x_{ij}$  as the sum of all Feynman parameters found between gluons  $i$  and  $j$ , when moving clockwise around the loop (see Fig. 2), so that, for example,  $x_{13} = x_1 + x_2$ . The complete expression for Eq. (4.3) in the field theory limit becomes then

$$\begin{aligned} A^{(1)}(p_1, p_2, p_3) &= N \operatorname{Tr}(\lambda^3 \lambda^2 \lambda^1) \frac{g_d^3}{(4\pi)^{d/2}} \int_0^\infty dt t^{2-d/2} \\ &\times \int_0^1 dx_1 dx_2 dx_3 \delta(1 - \sum_{j=1}^3 x_j) \\ &\times \exp \left[ -t (x_1 x_2 p_2^2 + x_2 x_3 p_3^2 + x_3 x_1 p_1^2) \right] \\ &\times \left\{ - \sum_{i=2,3; j=1,3; k=1,2} \epsilon_i \cdot p_i \epsilon_j \cdot p_j \epsilon_k \cdot p_k \right. \\ &\quad \left[ (d-2)(x_{1i} - x_{i1})(x_{2j} - x_{j2})(x_{3k} - x_{k3}) \right. \\ &\quad \left. + 8(x_{1i} - x_{i1} + x_{2j} - x_{j2} + x_{3k} - x_{k3}) \right] \\ &\quad + \sum_{(i,j,k)=(1,2,3),(2,3,1),(3,1,2)} \epsilon_i \cdot \epsilon_j \epsilon_k \cdot p_i \\ &\quad \left[ \frac{2(d-2)}{t} (x_{ik} - x_{ki}) + 16x_{ki} p_i \cdot p_j + 8p_j^2 \right] \\ &\quad + \sum_{(i,j,k)=(1,2,3),(2,3,1),(3,1,2)} \epsilon_i \cdot \epsilon_j \epsilon_k \cdot p_j \\ &\quad \left. \left[ \frac{2(d-2)}{t} (x_{jk} - x_{kj}) + 16x_{kj} p_i \cdot p_j + 8p_j^2 - 8p_k^2 \right] \right\}. \end{aligned} \quad (4.5)$$

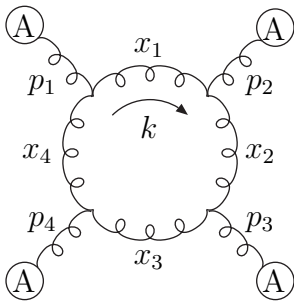


Figure 3: Four–point diagram: external gluons are background fields, marked by an A. Momenta  $p_i$  are incoming.

In writing Eq. (4.5), we kept all terms proportional to longitudinal gluon polarizations, but to get a symmetric expression we replaced, say,  $\epsilon_1 \cdot p_1$  with  $-\epsilon_1 \cdot p_2 - \epsilon_1 \cdot p_3$ . The result exactly matches the contribution of the corresponding color ordering to the three diagrams in Fig. 2, computed using the background field method, with the Feynman rules given for example in [22]<sup>5</sup>. We note in passing that the function appearing in the exponent of Eq. (4.5) depends only on the topology of the diagram, and thus is the same that would appear in a scalar theory.

Using symbolic algebraic manipulation programs, one can check at the level of integrands that our prescription gives the correct results for scalar graphs also for amplitudes with more gluons. We have tested the irreducible graph with only cubic vertices in the case of the four gluon amplitude, but the complete result is too lengthy to report here. It is more interesting to use the four–point amplitude as a testing ground for the computation of non–planar contributions, since the first non–trivial example arises in this case. Consider then the scalar graph containing the four–gluon diagram in Fig. 3, taking for simplicity on–shell gluons.

With a growing number of external particles, it is convenient to fix helicities, which helps to reduce the number of non–vanishing Lorentz invariant combinations of external momenta and polarizations. Using standard helicity techniques, we may choose for example the configuration  $\epsilon^+(p_1, p_4)$ ,  $\epsilon^+(p_2, p_4)$ ,  $\epsilon^-(p_3, p_1)$ ,  $\epsilon^-(p_4, p_1)$ , where the first argument is the external gluon momentum, while the second is the

<sup>5</sup>The string result must be multiplied by a factor  $i$ , since the string rules give directly the  $T$  matrix.

reference momentum, as explained in [2]. In this case the only five non-vanishing scalar products are  $\epsilon_2 \cdot \epsilon_3$ ,  $\epsilon_1 \cdot p_3 = -\epsilon_1 \cdot p_2$ ,  $\epsilon_2 \cdot p_1 = -\epsilon_2 \cdot p_3$ ,  $\epsilon_3 \cdot p_4 = -\epsilon_3 \cdot p_2$ , and  $\epsilon_4 \cdot p_2 = -\epsilon_4 \cdot p_3$ . Summing gluon and ghost loops, we find that the scalar graph, in the background field method, has the expression

$$\begin{aligned}
A^{(1)}(p_1, p_2, p_3, p_4) &= 8 i \mathcal{C} \frac{g_d^4}{(4\pi)^{d/2}} \int_0^\infty dt t^{3-d/2} \int_0^1 dx_1 dx_2 dx_3 dx_4 \delta(1 - \sum_{j=1}^4 x_j) \\
&\times \exp[t(s_{12}x_2x_4 + s_{23}x_1x_3)] (\epsilon_1 \cdot p_2)(\epsilon_4 \cdot p_3) \\
&\times \left\{ 2(\epsilon_2 \cdot p_3)(\epsilon_3 \cdot p_2) \left[ -2 x_2x_4 + (d-2)x_2^2(x_3 + x_4)(x_1 + x_4) \right] \right. \\
&\quad \left. + (\epsilon_2 \cdot \epsilon_3) \left[ s_{23} ((x_1 + x_3 + x_4)^2 + x_2^2) + (d-2)\frac{1}{t}x_2^2 \right] \right\}, \tag{4.6}
\end{aligned}$$

where the color factor is

$$\begin{aligned}
\mathcal{C} &= N [\text{Tr}(\lambda^1\lambda^2\lambda^3\lambda^4) + \text{Tr}(\lambda^4\lambda^3\lambda^2\lambda^1)] \\
&+ 2 [\text{Tr}(\lambda^1\lambda^2)\text{Tr}(\lambda^3\lambda^4) + \text{Tr}(\lambda^1\lambda^3)\text{Tr}(\lambda^2\lambda^4) + \text{Tr}(\lambda^1\lambda^4)\text{Tr}(\lambda^2\lambda^3)] . \tag{4.7}
\end{aligned}$$

Leading color terms can be obtained from the planar string amplitude, exactly as in the previous example. Here we focus on subleading terms proportional to double traces, which are reproduced by non-planar string amplitudes. They were absent in the three-point amplitude, since  $\text{Tr}(\lambda^i) = 0$ .

Consider, for example, the term proportional to  $\text{Tr}(\lambda^1\lambda^2)\text{Tr}(\lambda^3\lambda^4)$ . The string amplitude with this Chan-Paton factor is the one with  $z_1$  and  $z_2$  on one boundary (say, the positive real axis in the Schottky representation, Section 2, with  $z_1 = 1$ ) while  $z_3$  and  $z_4$  are on the other boundary. The non-planar master formula is similar to the planar one, with small but significant differences. First of all, when a Green function connects two punctures on different boundaries, its non-planar version, Eq. (3.5), must be used. Also, the correct expression for the projective transformations is  $V'_i(0) = |z_i|$ . Finally,  $z_2$  and  $z_3$  are not ordered, so that the resulting integration regions is the interval  $[-1, -k]$  for both punctures. To compare non-planar and planar contributions, we change variables according to  $z_3 \rightarrow -z'_3$  and  $z_4 \rightarrow -z'_4$ ; all punctures are now integrated on the positive real axis, just as in the planar case, however now it is necessary to distinguish six different orderings of the four punctures, namely

$$1) k \ll z'_4 \ll z'_3 \ll z_2 \ll 1$$

- 2)  $k \ll z_2 \ll z'_3 \ll z'_4 \ll 1$
- 3)  $k \ll z'_3 \ll z_2 \ll z'_4 \ll 1$
- 4)  $k \ll z'_4 \ll z_2 \ll z'_3 \ll 1$
- 5)  $k \ll z'_3 \ll z'_4 \ll z_2 \ll 1$
- 6)  $k \ll z_2 \ll z'_4 \ll z'_3 \ll 1$

Regions 1 and 2 correspond to the cyclic orderings  $(4-3-2-1)$  and  $(1-2-3-4)$ , respectively. The resulting integrands, expressed in terms of  $z_2$ ,  $z'_3$  and  $z'_4$ , are equal, but, at the string level, they differ from the planar amplitude. The difference, however, vanishes in the field theory limit, so the two regions add up to give the relative factor of 2 between the single trace planar contribution proportional to  $N\text{Tr}(\lambda^1\lambda^2\lambda^3\lambda^4)$  and the double trace contribution proportional to  $\text{Tr}(\lambda^1\lambda^2)\text{Tr}(\lambda^3\lambda^4)$  in Eq. (4.7).

Regions 3, 4, 5 and 6 correspond to the other cyclic orderings ( $(1-3-2-4)$ ,  $(1-4-2-3)$ ,  $(1-3-4-2)$ ,  $(1-2-4-3)$  respectively), so they are to be identified with the subleading terms of the other color-ordered field theory diagrams. This same mechanism has been observed for scalar diagrams [13]. The fact that the differences between planar and non-planar integrands vanish in the field theory limit is responsible for the relations between single trace and double trace subamplitudes, noticed already in [25].

## 5 Irreducible diagrams with quartic vertices

Quartic vertices arise in the field theory limit when the strong ordering condition between two punctures is relaxed. Changes of variables such as the one given in Eq. (4.1), in fact, generate a certain number of explicit powers of  $\alpha'$  in the integration measure. It is clear however, since Schwinger parameters are dimensionful, that there are potential  $\mathcal{O}(\alpha')$  corrections arising from regions of integration where the Schwinger parameters themselves, or their differences, are  $\mathcal{O}(\alpha')$ . Such corrections are negligible in a scalar theory, where all terms in the integrand have a uniform power of  $\alpha'$  when expressed in terms of the  $t_i$ 's; in a gauge theory amplitude, however, these terms do contribute, as explained in Section 3.

Suppose we want two consecutive punctures, say  $z_i$  and  $z_{i+1}$ , to attach to the loop through a quartic vertex: the propagator between them would have a Schwinger parameter proportional to  $t_{i+1} - t_i$ , so we must impose that this vanish in the

zero-slope limit, setting

$$t_{i+1} - t_i = \mathcal{O}(\alpha') \quad \Rightarrow \quad \frac{z_{i+1}}{z_i} \equiv y = \mathcal{O}(1) . \quad (5.1)$$

The correct procedure to take into account this region of integration is to change variables according to, say,  $z_i = \exp(-t_i/\alpha')$ , and  $z_{i+1} = y_i z_i$ , subsequently integrating over  $y_i$  in a neighborhood of  $y_i = 1$ . Notice that we now have a different overall power of  $\alpha'$ , since  $y_i$  is independent of  $\alpha'$ , so we will be considering a different set of terms in the expansion of the integrand in powers of  $\alpha'$ .

To define precisely the  $y_i$  integration, consider, for example, the integration region for the puncture  $z_2$ ,

$$\int_{z_3}^1 \frac{dz_2}{z_2} \rightarrow \frac{1}{\alpha'} \int_0^{t_3} dt_2 . \quad (5.2)$$

If we relax the condition of strong ordering of the punctures, we must explicitly consider regions in which  $t_2$  or  $t_3 - t_2$  are  $\mathcal{O}(\alpha')$ . In these regions the counting of powers of  $\alpha'$  is clearly different, as can be seen by writing

$$\frac{1}{\alpha'} \int_0^{t_3} dt_2 = \frac{1}{\alpha'} \int_0^{b\alpha'} dt_2 + \frac{1}{\alpha'} \int_{b\alpha'}^{t_3 - c\alpha'} dt_2 + \frac{1}{\alpha'} \int_{t_3 - c\alpha'}^{t_3} dt_2 , \quad (5.3)$$

where  $b$  and  $c$  are arbitrary  $\mathcal{O}(1)$  constants. The contribution of diagrams with three-point vertices, discussed in the previous section, arises from integrals such as the second term on the RHS of Eq. (5.3), where we pick the terms in the integrand that cancel the explicit factor of  $1/\alpha'$ , and thus we may neglect the  $\alpha'$  dependence in the limits of integration. The other two integrals in Eq. (5.3) do not have an overall power of  $\alpha'$ , because the size of the integration region vanishes with  $\alpha'$ . Defining  $t_2 = \alpha'\tau_1$  in the first integral, and  $t_3 - t_2 = \alpha'\tau_2$  in the second integral (corresponding to  $y_i = \exp(-\tau_i)$ ) we obtain

$$\frac{1}{\alpha'} \int_0^{t_3} dt_2 = \int_0^b d\tau_1 + \frac{1}{\alpha'} \int_{b\alpha'}^{t_3 - c\alpha'} dt_2 + \int_0^c d\tau_2 . \quad (5.4)$$

The  $b$  and  $c$  dependence arising from the upper limits of integration of the  $\tau$  integrals must cancel the dependence arising from the  $t_2$  integral when the limits of integration are expanded in powers of  $\alpha'$ . The correct treatment of the  $\tau_i$  integrations is thus to perform the integral exactly, but retain only the contribution from the lower limit of integration,  $\tau_i = 0$ , corresponding to  $y_i = 1$ . Notice that there is one (and only one) integration region of this kind for every propagator in the loop,

and the maximum number of regions that can simultaneously contribute is correctly given by the overall counting of powers of  $\alpha'$  in the string master formula, Eq. (2.6). Notice also that the choice of integration variables is built in the algorithm, since we are retaining only the contribution of one limit of integration: a generic change of variables, in particular a shift by a constant, will in fact redistribute the result of the integration between the two limits.

There is a class of terms contributing to scalar graphs with four-point vertices that requires regularization, as was already pointed out in Refs. [11] and [15]. These contributions arise when one takes  $z_{i+1}$  close to  $z_i$  in a term containing a double derivative of the Green function precisely with respect to these variables. Such terms diverge as  $z_{i+1} \rightarrow z_i$ , *i.e.*  $y_i \rightarrow 1$ , because of the double pole in  $\partial_i \partial_{i+1} G(z_i, z_{i+1})$ . To regularize this divergence, one may retain also the  $y$  dependence arising from the exponential of the same Green function, which is formally suppressed in the  $\alpha' \rightarrow 0$  limit. It's easy to see that the resulting integral is of the form

$$I(c, \alpha' p_i \cdot p_{i+1}) = \int_{e^{-c}}^1 dy (1-y)^{-2+2\alpha' p_i \cdot p_{i+1}} y^{-\alpha' p_i \cdot p_{i+1}} , \quad (5.5)$$

where  $c$  is the arbitrary constant defining the boundary of the appropriate integration region. Notice that there is some freedom concerning the inclusion of  $y$ -dependent terms arising from the exponential in this regularization prescription: in Eq. (5.5) we included exactly only the  $y$  dependence arising from  $G(z_i, z_{i+1})$ , while all other nonsingular terms (arising from, say,  $G(z_j, z_{i+1})$ , with  $j \neq i$ ) were dropped, to be treated according to the general rules outlined at the beginning of this section. As we will see in the next section, the inclusion of further  $y$ -dependent terms in Eq. (5.5) is equivalent to a reshuffling of one-particle-reducible and irreducible contributions to the amplitude.

The integral  $I(c, \alpha' p_i \cdot p_{i+1})$  is linearly divergent at the upper limit of integration when  $\alpha' \rightarrow 0$ , and requires regularization. It is comforting to verify that three independent regularization schemes give the same result in the field theory limit.

- The simplest approach is the one that was adopted in Refs. [11] and [15]. One can set  $\alpha' \rightarrow 0$  *ab initio* in Eq. (5.5), expand the integrand in powers of  $y$ , and integrate the series term by term, obtaining

$$I(c, 0) = \int_{e^{-c}}^1 \frac{dy}{(1-y)^2} = \int_{e^{-c}}^1 \frac{dy}{y} \sum_{n=1}^{\infty} n y^n = \sum_{n=1}^{\infty} y^n \Big|_{e^{-c}}^1 . \quad (5.6)$$

The lower limit contribution depends on  $c$ , so it must be discarded, as explained before. The remaining sum can be interpreted as a  $\zeta$ -function, yielding

$$\sum_{n=1}^{\infty} 1 = \lim_{s \rightarrow 0} \sum_{n=1}^{\infty} n^{-s} = \zeta(0) = -\frac{1}{2}. \quad (5.7)$$

This  $\zeta$ -function regularization was used in [15] also at the two-loop level, giving the correct field theory limit.

- Perhaps a more natural way to approach the regularization of Eq. (5.5) is to view it as an incomplete  $B$  function. As we shall see, this viewpoint nicely ties together diagrams with four-point vertices with reducible diagrams. Since our answer must be independent of  $c$ , we may turn the integral into an ordinary  $B$  function by taking the  $c \rightarrow \infty$  limit. Considering for simplicity a contribution to the two-point amplitude, and thus replacing  $p_i \cdot p_{i+1}$  with  $-p^2$ , we find

$$I(\infty, -\alpha' p^2) = B(-1 - 2\alpha' p^2, 1 + \alpha' p^2). \quad (5.8)$$

After analytic continuation we get  $I(\infty, 0) = -1/2$ , exactly as in Eq. (5.7).

- Finally, at one loop, these results are confirmed by integration by parts of double derivatives of the Green function, at the level of the string master formula, as was done in [11, 3]. After integration by parts, the correct field theory limit is obtained by considering only scalar graphs with cubic vertices, so that effectively the singularity we are studying is removed. The regularization given by Eq. (5.7) turns out to be the correct prescription to recover the same results without partial integration.

Our working prescription will then be

$$I(c, -\alpha' p^2) \rightarrow -\frac{1}{2}. \quad (5.9)$$

To illustrate the application of these rules, consider the diagram in Fig. 4, with off-shell and non-transverse gluons. To verify the correctness of our prescription, Eq. (5.9), we can focus on a specific kinematic structure, say  $\epsilon_1 \cdot \epsilon_2 \epsilon_3 \cdot p_4 \epsilon_4 \cdot p_2$ <sup>6</sup>.

---

<sup>6</sup>Notice that, in order to identify univocally the coefficients, we write  $\epsilon_3 \cdot p_3 = -\epsilon_3 \cdot p_1 - \epsilon_3 \cdot p_2 - \epsilon_3 \cdot p_4$  and  $\epsilon_4 \cdot p_4 = -\epsilon_4 \cdot p_1 - \epsilon_4 \cdot p_2 - \epsilon_4 \cdot p_3$ . The string master formula, in general, automatically generates the answer with this convention, which yields a particularly symmetric expression.



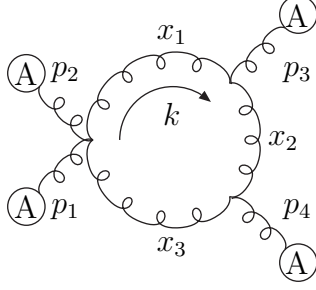


Figure 4: Four–point diagram with a quartic vertex: external gluons are background fields, marked by an A. Momenta  $p_i$  are incoming.

Setting  $z_2 = y$  in the master formula, Eq. (2.6) (recall that  $z_1 = 1$ ), we obtain

$$\begin{aligned}
A^{(1)}(p_1, p_2, p_3, p_4) &\rightarrow 8N \operatorname{Tr}(\lambda^4 \lambda^3 \lambda^2 \lambda^1) \frac{g_d^4}{(4\pi)^{d/2}} (\epsilon_1 \cdot \epsilon_2) (\epsilon_3 \cdot p_4) (\epsilon_4 \cdot p_2) \\
&\times \int_0^\infty dt t^{-d/2} \int_0^t dt_4 \int_0^{t_4} dt_3 \\
&\times \exp \left[ \frac{s_{12} t_3 (t - t_4) - p_3^2 t_3 (t_4 - t_3) - p_4^2 (t_4 - t_3) (t - t_4)}{t} \right] \\
&\times \frac{(2t_4 - t)(t - 2t_4 + 2t_3)}{4t^2} \\
&\times \int^1 \frac{dy}{y} \left[ \left( \frac{1}{y} + y \right) + (d-2) \frac{y}{(1-y)^2} \right], \tag{5.10}
\end{aligned}$$

where  $s_{12} = -2p_1 \cdot p_2$ , and we wrote only the relevant limit of integration in  $y$ . The term proportional to  $(1/y + y)$  integrates to zero, while for the term proportional to  $y/(1-y)^2$  we must use Eq. (5.9). The result for the contribution of the chosen kinematic structure to the scalar graph containing Fig. 4 is

$$\begin{aligned}
A^{(1)}(p_1, p_2, p_3, p_4) &\rightarrow N \operatorname{Tr}(\lambda^4 \lambda^3 \lambda^2 \lambda^1) \frac{g_d^4}{(4\pi)^{d/2}} (\epsilon_1 \cdot \epsilon_2) (\epsilon_3 \cdot p_4) (\epsilon_4 \cdot p_2) \\
&\times \int_0^\infty dt t^{-d/2+2} \int_0^1 dx_1 dx_2 dx_3 \delta(1 - \sum_{j=1}^3 x_j) \\
&\times \exp [t (s_{12} x_1 x_3 - p_3^2 x_1 x_2 - p_4^2 x_2 x_3)] \\
&\times ((2-d)(1-2x_2)(1-2x_3)) . \tag{5.11}
\end{aligned}$$

The result is again in agreement with the computation in the background field Feynman gauge, including the contribution of ghosts.

## 6 Reducible diagrams

Reducible diagrams (such as the one portrayed in Fig. 5) arise from the string master formula when two adjacent punctures, say  $z_i$  and  $z_{i+1}$ , are so close to each other on the world-sheet that the corresponding correlator,  $G(z_i, z_{i+1})$ , is dominated by its logarithmic short distance singularity even before the field theory limit is taken. In this integration corner, often called ‘pinching’ region [3], the string master formula effectively factorizes into the product of a one-loop amplitude with an off-shell leg, times a tree-level amplitude. All string states may flow through the propagator joining the two factors; the Yang–Mills field theory limit is reached by selecting the poles corresponding to the propagation of massless states.

As we will see, reducible diagrams are the only diagrams where it is necessary to require that a subset of the external legs (those forming the tree that attaches to the irreducible loop) be on-shell. This however is also a feature of diagrammatic computations in field theory when using the background field method [26]: there, reducible contributions to a scattering amplitude only coincide with the ones obtained with conventional methods provided all external legs on at least one side of the reducible propagator are put on shell.

The other relevant feature of the computation of reducible diagrams in the background field method, namely the possibility of using different gauges for the tree and the one-loop subamplitudes, is also preserved in string theory. In fact, our analysis will confirm the results obtained in [9] for on-shell diagrams and in [11] for the divergent part of off-shell diagrams with transverse gluons: the 1PI part of the diagram is expressed in the background field Feynman gauge, as expected from the previous sections; the tree part is computed by the string in a different gauge, the Gervais–Neveu gauge.

The Gervais–Neveu gauge is a non-linear gauge, introduced to analyze the field theory limit of open string theory [27]. The gauge-fixed action, ignoring ghosts, is:

$$S^{GN} = \int d^4x \left( -\frac{1}{2} \text{Tr}[F_{\mu\nu}^2] - \text{Tr}[(\partial \cdot A - igA^2)^2] \right). \quad (6.1)$$

The Feynman rules can be found, for example, in [5]. At tree level, the vertices are

simpler than those of the usual Feynman gauge, allowing efficient calculations. At one loop, the string still exploits this advantage in the tree part of the diagrams, but avoids the complications that ghost terms would generate if the gauge were used also for the one-loop part of the diagrams.

Reducible contributions can be extracted from the string master formula by considering the region of moduli space where  $z_i - z_{i+m} \ll k \rightarrow 0$  [3, 11]. To start with, we consider the case  $i = m = 1$ , where, as in the previous section,  $z_2 \rightarrow z_1 = 1$ . In this limit the string amplitude naturally factorizes in a sum over poles which correspond to the propagation of different string states in a ‘reducible’ leg connecting two separate parts of the diagram. We have already studied the contribution of the first term of this sum, which is related to the exchange the tachyonic ground state. With either of the two regularizations proposed, (5.7) or (5.8), one recovers contributions to the irreducible diagram depicted in Fig. (4).

The basic idea of the ‘pinching’ procedure adopted in [3, 11] is to associate the contribution due to the exchange of massless states to reducible diagrams. In order to select the appropriate pole for the massless exchange one has to perform a Taylor expansions in  $z_{i+j}$  around  $z_i$  of all string Green functions (3.4). However, for the ‘pinched’ legs, which are isolated on a reducible tree, we use an effective Green function determined only by the short distance behavior of the string expression, which is equal to the tree-level Green function,

$$G^E(z_i, z_j) = \log |z_i - z_j|. \quad (6.2)$$

As an example, let us consider the reducible diagram in Fig. 5, where we have to assume that legs 1 and 2 are on shell, as explained above. Taking the limit  $z_2 \rightarrow 1$  by means of Eq. (6.2), we observe that the exponential involving  $G(z_1, z_2)$  yields a factor of  $(1 - z_2)^{-\alpha' s_{12}}$ , while further factors of  $(1 - z_2)$  can be generated by expanding the other Green functions and their derivatives around  $z_2 = 1$ ; for example,

$$\begin{aligned} G_{32} &\xrightarrow{z_2 \rightarrow 1} G_{31} + (1 - z_2) \left[ -\frac{1 + z_3}{2(1 - z_3)} + \frac{\log z_3}{\log k} + k \frac{1 - z_3^2}{z_3} \right], \\ \partial_3 G_{32} &\xrightarrow{z_2 \rightarrow 1} \partial_3 G_{31} + (1 - z_2) \left[ -\frac{1}{(1 - z_3)^2} + \frac{1}{z_3 \log k} - k \frac{(1 + z_3^2)}{z_3^2} \right], \\ \partial_2 \partial_3 G_{32} &\xrightarrow{z_2 \rightarrow 1} \partial_2 \partial_3 G_{32}|_{z_2=1} + (1 - z_2) \left[ -\frac{2}{(1 - z_3)^3} - \frac{1}{z_3 \log k} - 2k \right], \end{aligned} \quad (6.3)$$

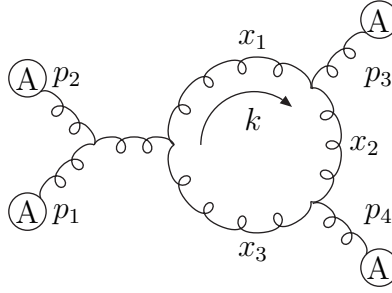


Figure 5: Reducible four–point diagram: external gluons are background fields, marked by an A. Momenta  $p_i$  are incoming.

where terms of order  $\mathcal{O}((1 - z_2)^2)$  and  $\mathcal{O}(k^2)$  have been neglected. Clearly, Taylor–expanding in powers of  $(1 - z_2)$  generates a series of poles in the  $s_{12}$  channel; in fact, the general integral in  $z_2$  is of the form

$$\int_{z_3}^1 dz_2 (1 - z_2)^{-\alpha' s_{12} + a - 1}, \quad (6.4)$$

with integer  $a$ . Since  $z_3 \rightarrow 0$  exponentially as  $\alpha' \rightarrow 0$ , we can evaluate the integral (possibly by analytic continuation in the external momenta) as

$$\int_0^1 dz_2 (1 - z_2)^{-\alpha' s_{12} + a - 1} = (a - \alpha' s_{12})^{-1}. \quad (6.5)$$

Different values of  $a$  correspond to different mass eigenstates propagating in the  $s_{12}$  channel. For example,  $a = -1$  corresponds to tachyon propagation, which we now discard, while the expected gluon pole  $1/s_{12}$  is given by  $a = 0$ . Notice that, as announced, we have to require  $p_1$  and  $p_2$  to be on shell in order to rewrite  $2p_1 \cdot p_2$  as  $-s_{12}$ . Having isolated the massless pole, one may apply the procedure illustrated in Section 3 and Section 4 (only cubic vertices are connected to the loop in this case) and get the correct expression for the diagram in Fig. 5. For example, selecting the term  $(\epsilon_1 \cdot \epsilon_2)(\epsilon_3 \cdot p_4)(\epsilon_4 \cdot p_2)$ , one finds

$$A^{(1)}(p_1, p_2, p_3, p_4) \rightarrow g_d^4 N \text{Tr}(\lambda^4 \lambda^3 \lambda^2 \lambda^1) \frac{2}{(4\pi)^{d/2}} (\epsilon_1 \cdot \epsilon_2)(\epsilon_3 \cdot p_4)(\epsilon_4 \cdot p_2) \quad (6.6)$$

$$\times \int_0^\infty dt t^{-d/2+2} \int_0^1 dx_1 dx_2 dx_3 \delta(1 - \sum_{j=1}^3 x_j)$$

$$\begin{aligned}
& \times \exp [t(s_{12}x_1x_3 - p_3^2x_1x_2 - p_4^2x_2x_3)] \tag{6.7} \\
& \times \frac{1}{s_{12}} \{2(d-2)(1-2x_2)t^{-1} - 8[p_1 \cdot p_3 + p_1 \cdot p_4(1-2x_2)] \\
& \quad + (d-2)(1-2x_2)(1-2x_3)[p_2 \cdot p_3(1-2x_1) - p_2 \cdot p_4(1-2x_3)]\} .
\end{aligned}$$

The approach just described has a simple diagrammatic interpretation and, in particular, it has the advantage of clearly separating reducible and irreducible contributions. However, the use of an *ad-hoc* Green function, Eq. (6.2), may appear arbitrary and not completely justified at the string level. Here we want to outline also an alternative method for computing reducible diagrams, which is a natural extension of our rules for the calculation of diagrams with four-point vertices. As we will show, in this case one does not have to introduce any effective Green functions. On the contrary, it is sufficient to introduce the parameter  $y = z_2/z_1$ , as in Eq. (5.1), and to carefully study the region  $y = 1$ . Using this second method, diagrams with quartic vertices and reducible diagrams are computed simultaneously.

The starting point of the alternative method is a natural generalization of the regularization (5.8) presented in Section 5. In particular, one has to retain all logarithmic dependence on  $y$  in the exponential containing the sum of Green functions. In this way, one finds a term of the form

$$\mathcal{Y}(y) = (1-y)^{2\alpha'p_1 \cdot p_2} y^{-\alpha'p_1 \cdot p_2 + \alpha'p_2 \cdot p_3(1-2\frac{t_3}{t}) + \alpha'p_2 \cdot p_4(1-2\frac{t_4}{t})} , \tag{6.8}$$

which gives a natural regularization of the tachyonic divergence  $(1-y)^2$ . The  $t$ 's above are the Schwinger parameters related in the usual way to the string variables:  $t_3 = -\alpha' \log z_3$ ,  $t_4 = -\alpha' \log z_4$  and  $t = -\alpha' \log k$ . As explained in Section 5, for regular terms we perform the  $y$  integral exactly, keeping only the contribution of the  $y = 1$  limit of integration. In this case, the factor (6.8) has no effect on the integration. For singular terms, we obtain a generalization of Eq. (5.5). In particular, the tachyonic double pole at  $y \rightarrow 1$  gives the contribution

$$\begin{aligned}
& \int_{e^{-c}}^1 dy (1-y)^{-2} \mathcal{Y}(y) \rightarrow \int_0^1 dy (1-y)^{-2} \mathcal{Y}(y) \\
& = B \left( -1 + 2\alpha'p_1 \cdot p_2, 1 - \alpha'p_1 \cdot p_2 + \alpha'p_2 \cdot p_3 \left( 1 - 2\frac{t_3}{t} \right) + \alpha'p_2 \cdot p_4 \left( 1 - 2\frac{t_4}{t} \right) \right) \\
& = -\frac{1}{2} - \frac{1}{2p_1 \cdot p_2} \left[ p_2 \cdot p_3 \left( 1 - 2\frac{t_3}{t} \right) + p_2 \cdot p_4 \left( 1 - 2\frac{t_4}{t} \right) \right] + \mathcal{O}(\alpha') . \tag{6.9}
\end{aligned}$$

Of course, Eq. (6.9) is just a factor of the amplitude; to recover the complete result one has to include the appropriate measure of integration and the exponential

factor appearing in Eq. (5.10), which encode the contribution coming from the punctures not involved in the pinching procedure. It is easy to see that the first term reproduces the prescription we introduced in Eq. (5.9) to get the irreducible diagram with a quartic vertex, Fig. 4; the other terms, containing a pole in  $2p_1 \cdot p_2$ , contribute to the reducible configuration, Fig. 5.

Simple poles in  $(1 - y)$  must be treated in exactly the same way, obtaining again

$$\int_{e^{-c}}^1 dy (1 - y)^{-1} \mathcal{Y}(y) = \frac{1}{2\alpha' p_1 \cdot p_2} + \mathcal{O}((\alpha')^0), \quad (6.10)$$

which is another contribution to the reducible diagram. Notice the negative power of  $\alpha'$  in Eq. (6.10): it tells us that we need to consider also contributions of order  $\alpha'$ , obtainable from the expansion of the exponential, as outlined in Eq. (3.3); furthermore, one must expand around  $y = 1$  all the terms multiplying Eq. (6.8), to be sure to get all terms of the type (6.10). The difference with the previous approach is that here we kept the exact dependence on  $y = z_2$  in all exponentiated Green functions and no expansion in  $y$  was done in the terms proportional to  $\log(y)$ , present, for instance, in  $G_{23}$ . Because of this, the contribution of the simple pole is now different from the one of Eq. (6.7) and in particular the last term proportional to  $(d - 2)$  is absent. The complete result is recovered only once one takes into account the reducible contribution coming from the new regularization (6.9).

The first method is maybe preferable from the computational point of view, because it preserves the one-to-one correspondence between string regions and Feynman graphs. The second method, on the other hand, is interesting because it ties together the prescription for quartic vertices, Eq. (5.9), and the one for reducible diagrams.

It is not difficult to generalize the method we just presented to more complicated situations where the pinching procedure involves two non-consecutive legs, like  $z_i$  and  $z_{i+m}$ . In this case, the role of the variable  $y$  is taken by the combination  $z_{i+m}/z_i$ . Moreover, one can introduce the variables  $\zeta_l = (z_{i+l} - z_{i+m})/(z_i - z_{i+m})$  for  $l = 1, 2, \dots, m - 1$ , which factorize the expression of the amplitude in two separate parts. The term depending only on the  $\zeta$ 's has the functional form of a tree-level amplitude and describes the legs isolated in the reducible part, while the other term of the amplitude can be treated as usual and gives the contribution of the irreducible part.

## 7 Systematics

We have completed the list of all regions of string moduli space contributing to the Yang–Mills field theory limit of the string master formula. Each region corresponds to a scalar graph of a given topology, and we have given a procedure to compute the corresponding contribution to the field theory amplitude in each case. We emphasize that all steps in the computation may be automated, in a manner essentially independent of the number of external gluons. In the special, but phenomenologically most relevant case of on–shell scattering amplitudes, the steps of the calculation of a given one–loop multigluon amplitude can be summarized as follows.

- Use color and helicity decomposition techniques to reduce the computation of the full amplitude to its basic building blocks, color–ordered fixed–helicity subamplitudes. For each independent subamplitude, choose polarization vectors to minimize the number of non–zero scalar products of polarizations and momenta.
- List all scalar graphs contributing to the full amplitude, *i.e.* all one–loop graphs that would contribute to the corresponding amplitude in a scalar theory with cubic and quartic vertices. Because the answer will be given in dimensional regularization, graphs that vanish in that scheme (such as tadpoles and bubbles on massless external legs) need not be included.
- Each subamplitude can now be written as a sum over scalar graphs,

$$A_{\{\lambda_i\},\mathcal{C}}^{(1)}(1,\dots,M) = \frac{g_d^M}{(4\pi)^{2-\epsilon}} \int_0^\infty dt t^{-2+\epsilon} \sum_g \int_0^1 \prod_{i=1}^{n_g} dx_i \delta\left(1 - \sum_{j=1}^{n_g} x_j\right) \times \exp\left[-tS_g(x_i; p_i \cdot p_j)\right] R_g\left(t, x_i; p_i, \epsilon_i^{(\lambda_i)}\right), \quad (7.1)$$

where the subscript  $\mathcal{C}$  denotes the color structure whose coefficient we are computing, and  $n_g$  is the number of propagators in the scalar graphs  $g$  contributing to the amplitude. The dynamical information is encoded in the functions  $S_g$  and  $R_g$ , which can be computed according to the rules given in the previous sections. Specifically,  $S_g$  is the same function of external momenta and Schwinger parameters that would appear in a scalar theory for a graph with the same topology; thus, it can be easily computed in field theory

as well as derived from string theory. The non-trivial content of Yang–Mills subamplitudes is given by the function  $R_g$ , which is a sum of polynomials in the dimensionless Schwinger parameters  $x_i$ , multiplied times integer powers of  $t$ . As a consequence, the  $t$  integration can always be done at the outset, yielding a  $\Gamma$  function. Using helicity techniques from the beginning will, in general, greatly simplify the function  $R_g$ , which in fact will vanish for many graphs for each subamplitude.

- Perform Schwinger parameter integrals. At this stage, string theory can offer no further help; techniques have been developed [28], however, that are sufficient to compute all one-loop scalar integrals that might be needed for Yang–Mills amplitudes in the foreseeable future.

The method just outlined allows, as is well known, to take advantage of the best organization of the amplitude in terms of color and helicity decompositions. The dimensional regularization scheme which naturally emerges in this approach is the so-called 't Hooft–Veltman scheme [29]: polarizations of external, observed gluons are in four dimensions, while polarizations of gluons circulating in the loop or otherwise unobserved are in  $d = 4 - 2\epsilon$  dimensions, as indicated by the factor  $(1 + k(d - 2))$  of Eq. (4.3). It should perhaps be further emphasized that a major practical advantage for amplitudes with several gluons is the fact that loop momentum integration has already been performed. To illustrate this fact, consider the six-gluon diagram in Fig. 6 (with all gluons on-shell and transverse).

Using Feynman rules and introducing Schwinger parameters, this diagram by itself generates approximately  $10^4$  terms, each of which must still be integrated over the loop momentum  $k$ . Suppose we focus on a particular kinematical structure, say  $\epsilon_1 \cdot \epsilon_5 \epsilon_2 \cdot \epsilon_6 \epsilon_3 \cdot p_5 \epsilon_4 \cdot p_5$ <sup>7</sup>: for most of the original  $10^4$  terms, this kinematical structure is generated only upon loop momentum integration, so while we can postpone integration over Schwinger parameters, we must integrate all terms in  $k$ . Methods to perform these integrals are well-known [23], but they generate larger and larger expressions as the power of  $k$  grows; in the present case, each contribution with 6 powers of  $k$  can generate up to  $6 \cdot 10^5$  terms. When all is said and done, the coef-

---

<sup>7</sup>Notice that for transverse gluons not all products  $\epsilon_i \cdot p_j$  for fixed  $i, i \neq j$ , are independent. To pick a basis, we choose to eliminate the products  $\epsilon_3 \cdot p_6$  and  $\epsilon_4 \cdot p_6$  using momentum conservation. The kinematic structure considered is present, for example, in the six-gluon amplitudes with helicities fixed as  $\epsilon^-(p_1, p_4), \epsilon^-(p_2, p_4), \epsilon^-(p_3, p_4), \epsilon^+(p_4, p_3), \epsilon^+(p_5, p_3), \epsilon^+(p_6, p_3)$ .



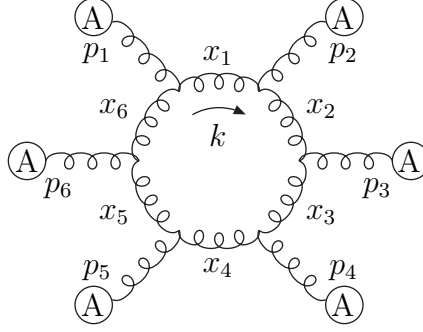


Figure 6: Six–point diagram: external gluons are background fields, marked by an A. Momenta  $p_i$  are incoming.

ficient of the chosen kinematical structure must be picked out of more than  $4 \cdot 10^6$  terms, and that applies to just one diagram. Clearly, this is a time and memory consuming task.

The string technique avoids all this. The change of variables identifying the field theory limit for a given scalar graph is known a priori, and all subsequent computerized manipulations involve only algebraic operations and series expansions. Using a symbolic manipulation program, such as Mathematica, on a normal PC, the Feynman parameter integrand for a given scalar graph, such as the one containing Fig. 6 and the corresponding ghost loops, can be obtained in seconds. In this case, for example, computing the coefficient of the chosen kinematic structure in the color–ordered amplitude multiplying  $\text{Tr}(\lambda^6 \dots \lambda^1)$  yields

$$\begin{aligned}
S_g(x_i; p_i \cdot p_j) &= 2p_1 \cdot p_2 x_2 x_6 + 2p_2 \cdot p_3 x_1 x_3 + 2p_3 \cdot p_4 x_2 x_4 + 2p_4 \cdot p_5 x_3 x_5 \\
&+ 2p_5 \cdot p_6 x_4 x_6 + 2p_6 \cdot p_1 x_1 x_5 + (p_1 + p_2 + p_3)^2 x_3 x_6 \\
&+ (p_2 + p_3 + p_4)^2 x_1 x_4 + (p_3 + p_4 + p_5)^2 x_2 x_5 , \tag{7.2}
\end{aligned}$$

and

$$\begin{aligned}
R_g(t, x_i; p_i, \epsilon_i) &= 16t^3 x_5 \left[ (d-2)x_5 - 2t(p_1 \cdot p_3 + p_1 \cdot p_4 - p_2 \cdot p_3 - p_2 \cdot p_4) \right. \\
&\left. - 4t x_5 (p_1 \cdot p_5 + p_2 \cdot p_6) \right] \epsilon_1 \cdot \epsilon_5 \epsilon_2 \cdot \epsilon_6 \epsilon_3 \cdot p_5 \epsilon_4 \cdot p_5 + \dots . \tag{7.3}
\end{aligned}$$

Needless to say, the result in Eq. (7.3) agrees with the corresponding background field method calculation.

## 8 Concluding remarks

We have completed a systematic analysis detailing how the one-loop string moduli space splits into particle graphs in the field theory limit. For each class of graphs, a specific  $\alpha'$ -dependent change of variables has been introduced, which parametrizes the limiting process to be implemented on the integrand of the string master formula. We have given a geometric prescription for the choice of projective transformations associated with external particles, so that our formulas apply to off-shell, arbitrarily polarized gluons, and can be used directly to compute general gluon correlation functions, in a manner which is completely alternative to, though much more efficient than conventional Feynman rules, at least at one loop. Singularities arising at the boundaries of different regions of moduli space have been consistently regulated, so as to avoid double counting. The method as it stands can be implemented in computer code using available symbolic manipulation programs. Such a program would be able to compute one-loop Yang-Mills amplitudes and gluon correlation functions, starting from the string master formula, provided the relevant Schwinger parameter integrals are known in dimensionally regularized form.

An obvious application of the method is the computation of one-loop scattering amplitudes with several gluons, which are relevant for next-to-leading order corrections to multijet production at hadron colliders. Such amplitudes are known for up to five gluons [30]; the six-gluon amplitude remains quite challenging even with the present technology, but it is a natural and interesting testing ground; in particular, it could be used to construct finite predictions for NLO partonic cross sections, since the seven-gluon tree-level amplitude is known in closed form [31].

Other possible applications arise from the fact the method can be applied off shell. At tree level, amplitudes with one off-shell gluon are related to currents [32], which can be exploited to establish recursion relations for the calculation of on-shell matrix elements. For certain classes of diagrams, these recursion relations have been generalized to one loop [33], but the complete extension including diagrams with gluon loops is not known. The present formalism would appear to be a natural framework to pursue this kind of generalization. Other areas of interest include the study of the high-energy, collinear and infrared limits of the amplitudes. For example, since one can now use string theory to compute matrix elements uncontracted with polarization vectors, it would be interesting to attempt a ‘stringy’ derivation

of the soft gluon current, recently derived at one loop by conventional methods [34].

Finally, we believe that the present systematic study is a necessary step for the extension of the method to more than one loop. As was shown in the case of scalar field theories, at two loops the decomposition of string moduli space into particle graphs is much more intricate than at one loop, even when considering only diagrams with cubic vertices [13]. A thorough understanding of the one-loop case on a graph by graph basis, including the non-trivial case of diagrams with four point vertices, will be of considerable help in the study of more complicated graph topologies.

## Acknowledgements

We would like to thank C. Schubert for several useful observations. R.R. acknowledges the support of the European Commission RTN programme HPRN-CT-2000-00131 and of the Physics Department of the University of Neuchâtel, where part of this work was carried out. L.M. acknowledges the support of the European Commission TMR programme FMRX-CT98-0194 (DG 12 - MIHT). Work supported in part by the italian Ministero dell'Università e della Ricerca Scientifica.

## References

- [1] A. Neveu and J. Scherk, *Nucl. Phys.* **B36** (1972) 155.
- [2] M.L. Mangano and S.J. Parke, *Phys. Rep.* **200** (1991) 301.
- [3] Z. Bern and D.A. Kosower, *Phys. Rev.* **D38** (1988) 1888; *Phys. Rev. Lett.* **66** (1991) 1669; *Nucl. Phys.* **B379** (1992) 451;
- [4] Z. Bern, *Phys. Lett.* **B296** (1992) 85.
- [5] Z. Bern, in *Proceedings of TASI 92*, eds. J. Harvey and J. Polchinski, [hep-ph/9304249](#); Z. Bern, L. Dixon and D.A. Kosower, *Ann. Rev. Nucl. Part. Sci.* **46** (1996) 109, [hep-ph/9602280](#).
- [6] For a review, see C. Schubert “Perturbative Quantum Field Theory in the String-Inspired Formalism”, preprint **LAPTH-761/99**, to appear in *Phys. Rep.*, and references therein.

- [7] L. Cappiello, R. Marotta, R. Pettorino and F. Pezzella, *Mod. Phys. Lett.* **A13** (1998) 2433, [hep-th/9804032](#); *Mod. Phys. Lett.* **A13** (1998) 2845, [hep-th/9808164](#); A. Liccardo, R. Marotta and F. Pezzella, *Mod. Phys. Lett.* **A14** (1999) 799, [hep-th/9903027](#); F. Cuomo, R. Marotta, F. Nicodemi, R. Pettorino, F. Pezzella and G. Sabella, [hep-th/0011071](#).
- [8] O. Andreev and H. Dorn, *Nucl. Phys.* **B583** (2000) 145, [hep-th/0003113](#); A. Bilal, C. Chu and R. Russo, *Nucl. Phys.* **B582** (2000) 65, [hep-th/0003180](#); C. Chu, R. Russo and S. Sciuto, *Nucl. Phys.* **B585** (2000) 193, [hep-th/0004183](#).
- [9] Z. Bern and D.C. Dunbar, *Nucl. Phys.* **B379** (1992) 562.
- [10] P. Di Vecchia, A. Lerda, L. Magnea and R. Marotta, *Phys. Lett.* **B351** (1995) 445, [hep-th/9502156](#).
- [11] P. Di Vecchia, L. Magnea, A. Lerda, R. Russo and R. Marotta, *Nucl. Phys.* **B469** (1996) 235, [hep-th/9601143](#).
- [12] P. Di Vecchia, L. Magnea, A. Lerda, R. Marotta and R. Russo, *Phys. Lett.* **B388** (1996) 65, [hep-th/9607141](#).
- [13] A. Frizzo, L. Magnea and R. Russo, *Nucl. Phys.* **B579** (2000) 379, [hep-th/9912183](#).
- [14] R. Marotta and F. Pezzella, *Phys. Rev.* **D61** (2000) 106006, [hep-th/9912158](#); see also [hep-th/0003044](#).
- [15] L. Magnea and R. Russo, in *Proceedings* of “DIS 97”, Chicago, USA, 1997, eds. J. Repond and D. Krakauer, AIP Conf. Proc. n. 407, 913, [hep-ph/9706396](#); also in *Proceedings* of “Beyond the Standard Model V”, Balholm, Norway, 1997, eds. G. Eigen, P. Osland and B. Stugu, AIP Conf. Proc. n. 415, 347, [hep-ph/9708471](#).
- [16] B. Kors and M.G. Schmidt, [hep-th/0003171](#).
- [17] J. Gomis, M. Kleban, T. Mehen, M. Rangamani and S. Shenker, *JHEP* **0008** (2000) 011, [hep-th/0003215](#).

- [18] See, for example, P. Di Vecchia, “*Multiloop amplitudes in string theory*” in Erice, *Theor. Phys.* (1992), 16, and references therein.
- [19] M.B. Green, J.H. Schwarz and E. Witten, “*Superstring Theory*”, Cambridge University Press (1987).
- [20] P. Di Vecchia, F. Pezzella, M. Frau, K. Hornfeck, A. Lerda and S. Sciuto, *Nucl. Phys.* **B322** (1989) 317.
- [21] K. Roland, *Phys. Lett.* **B289** (1992) 148.
- [22] L.F. Abbott, *Nucl. Phys.* **B185** (1981) 189.
- [23] G. Passarino and M. Veltman, *Nucl. Phys.* **B160** (1979) 151.
- [24] W.L. van Neerven and J.A.M. Vermaseren, *Phys. Lett.* **B137** (1984) 241.
- [25] Z. Bern and D.A. Kosower, *Nucl. Phys.* **B362** (1991) 389.
- [26] L.F. Abbott, M.T. Grisaru and R.K. Schaefer, *Nucl. Phys.* **B229** (1983) 372.
- [27] J.L. Gervais and A. Neveu, *Nucl. Phys.* **B46** (1972) 381.
- [28] Z. Bern, L. Dixon and D.A. Kosower, *Nucl. Phys.* **B412** (1994) 751, hep-ph/9306240; T. Binoth, J.Ph. Guillet, G. Heinrich, *Nucl. Phys.* **B 572** (2000) 361, hep-ph/9911342.
- [29] G. 't Hooft and M. Veltman, *Nucl. Phys.* **B44** (1972) 189; S. Catani, M.H. Seymour and Z. Trócsányi, *Phys. Rev.* **D55** (1997) 6819, hep-ph/9610553.
- [30] Z. Bern, L. Dixon and D.A. Kosower, *Phys. Rev. Lett.* **70** (1993) 2677, hep-ph/9302280.
- [31] R. Kleiss and H. Kuijf, *Nucl. Phys.* **B312** (1989) 616.
- [32] F.A. Berends and W. Giele, *Nucl. Phys.* **B306** (1988) 759.
- [33] G. Mahlon, *Phys. Rev.* **D49** (1994) 4438, hep-ph/9312276; in “Beyond the Standard Model 4”, Lake Tahoe 1994, 475, hep-ph/9412350.
- [34] S. Catani and M. Grazzini, *Nucl. Phys.* **B591** (2000) 435, hep-ph/0007142.